A Comparison of Artifact Reduction Methods for Real-Time Analysis of fNIRS Data

Takayuki Nozawa and Toshiyuki Kondo

Institute of Symbiotic Science and Technology, Tokyo University of Agriculture and Technology, 2-24-16 Naka-cho, Koganei-shi, Tokyo 184-8588, Japan
{tknozawa,t_kondo}@cc.tuat.ac.jp

Abstract. Due to its convenient, low physical restraint, and electric noise tolerant features, functional near-infrared spectroscopy (fNIRS) is expected to be a useful tool in monitoring users' brain activity in HCI. However, fNIRS measurement suffers from various kinds of artifacts, and no standardized method for artifact reduction has been established so far. In this study, we compared high-pass/band-pass filtering, global and local average references, independent component analysis (ICA) based method, and their combinations. Their effectiveness for artifact reduction was evaluated by a cognitive task recognition experiment. The results showed all the methods have artifact reduction capability, but their effectiveness depends on subjects and tasks. This suggests that it can be more practical to try various artifact reduction methods and chose the best one for each task and subject, instead of pursuing a single standardized method.

1 Introduction

Human computer interactions, including mobile interactions, are beginning to incorporate wide range of sensors for detection of user intention and context, from GPS and accelerometer to the sensors of various biomedical signals. Among them, sensing users' brain activity is expected to provide rich information for HCI, and being studied extensively in the field of brain-computer interface (BCI) or brain-machine interface (BMI). There, brain activity data are analyzed and classified in real-time, and the result is used for identification and monitoring of the user's cognitive states or for control of devices, etc. While electroencephalography (EEG) is most widely utilized in non-invasive BCI, usefulness of functional near-infrared spectroscopy (fNIRS) as a convenient, low physical restraint, and electric noise tolerant method, is worth to be studied more intensely for HCI and mobile interactions. (For example, HITACHI Inc. has developed a "wearable optical topography" system that facilitates study of brain activity in daily life [1].)

Like the functional magnetic resonance imaging (fMRI), fNIRS evaluates neural activity indirectly from blood-flow change in cortical microvasculature. This brings some difficulty in real-time analysis and utilization of fNIRS data for BCI. For one thing, the temporal resolution is said to be not very high (several seconds in time scale), due to relatively large time constant in neurovascular coupling. However, it

M.J. Smith and G. Salvendy (Eds.): Human Interface, Part II, HCII 2009, LNCS 5618, pp. 413–422, 2009.

has recently been reported that quicker (≤ 100 milliseconds in time scale) component may also reflect changes in cognitive tasks [2].

Another difficulty from the measurement mechanism of fNIRS is the existence of blood flow artifacts that do not originate in cognitive activity of the brain. Periodic components corresponding to cardiac, respiratory and other blood-flow regulation dynamics are frequently observed [3, 4]. Changes in posture, such as tilting the head, often induce relatively large artifacts on the fNIRS data (given that the measurement optodes are well settled, this is likely to be due to skin blood concentration or dispersion by gravity). Hence naive analysis of fNIRS data from an experiment without any posture regulation can result in a spurious correlation, which is in fact caused by body movement accompanied by task execution. However, neither posture regulation nor systematic artifact reduction has been mentioned in some literature on fNIRS studies. Continued pressure and heating by optodes occasionally induce a drift component. In some HCI applications, slow components derived from change in arousal level or mental fatigue should be distinguished as artifacts, even though they are associated with brain activity.

These types of artifacts are commonly expected in the application for HCI, and besides, even in the same measurement setting, the existence and magnitude of these artifacts are considerably different among subjects. In the current study, we focus on this problem, and study the effectiveness of several artifact reduction methods which are available for real-time analysis.

2 Method

In this section, we briefly review the basis of fNIRS measurement mechanism, and then describe the artifact reduction methods that we tested.

2.1 fNIRS

Transmission of near-infrared light in living tissue is sensitive to hemoglobin concentration and oxygenation state, with different absorption characteristics for different wavelengths. Using this physical property, fNIRS estimates changes in hemoglobin concentration associated with changes in regional cerebral blood flow (rCBF), which are coupled to those in neuronal activity [5].

We use an fNIRS imaging system (FOIRE-3000, Shimadzu Co., Japan), which adopts near-infrared lasers of thee wavelengths, 780, 805, and 830 nm. For each channel j (that corresponds to a neighboring pair of source and detector optodes, as shown in Fig. 1), optical densities $A_{j,\lambda}$ in wavelengths λ are measured. Then, from the changes in the optical density $\Delta A_{j,\lambda}$, relative concentration changes of oxygenated hemoglobin Δoxy_j and of deoxygenated hemoglobin $\Delta deoxy_j$ are estimated by

$$\begin{pmatrix} \Delta oxy_j \\ \Delta deoxy_j \end{pmatrix} = \begin{pmatrix} -1.4877 & 0.5970 & 1.4877 \\ 1.8545 & -0.2394 & -1.0947 \end{pmatrix} \begin{pmatrix} \Delta A_{j,780} \\ \Delta A_{j,805} \\ \Delta A_{j,830} \end{pmatrix}, \tag{1}$$

which is derived from the modified Beer-Lambert law and the extinction coefficients of the tissue reported by Matcher et al. [6, 7].

2.2 Artifact Reduction Methods

As artifact reduction methods, we picked up high-pass/band-pass filtering, global and local average references, independent component analysis (ICA), and their combinations.

High-pass/Band-pass Filtering. *High-pass filter* and *band-pass filter* have been frequently used in offline analysis of fNIRS data, to eliminate drift component and flatten the baseline (in the case of band-pass filter, also to eliminate quick components and smooth the data) [8-10]. In these cases, the filtering has been applied in the frequency domain, attaining virtually ideal brick-wall filter. For real-time analysis, however, a causal filter must be used, though it entails the risk of phase shift and distortion.

One should note that the cutoff frequency must be chosen according to the setting of HCI tasks. In our experimental setting, as explained in Section 3, fNIRS recording lasted about 10 minutes and high-frequency components were averaged out for the performance evaluation of artifact reduction. Therefore, aiming at reducing only slow artifact components (especially the drift which can be induced by change of arousal level, fatigue, continued warming, etc.), we used 4th order Butterworth high-pass filter [11], with cutoff frequency 1.67×10^{-3} Hz.

Global Reference. If an artifact component is assumed to be added uniformly on wide range of channels, it can be reduced by subtracting the global average across all the channels from the raw data of each channel in every time. This *global reference* method can be also effective in extracting localized brain response, and has often been used for EEG data (e.g. [12]).

As the concentration changes Δoxy_j and $\Delta deoxy_j$ are relative quantities, direct comparison or averaging of those values among channels can cause false results. One way to avoid this problem is to convert the raw data from each channel into the z-score in advance [13]: First, mean and standard deviation (SD) of $(\Delta oxy_j, \Delta deoxy_j)$ in "preparation phase" of a measurement are calculated for each channel j, as $(\mu_j^{\Delta oxy}, \mu_j^{\Delta deoxy})$ and $(\sigma_j^{\Delta oxy}, \sigma_j^{\Delta deoxy})$. Using these values, every data at time t in "analysis (testing) phase", as well as data in the preparation phase, are converted by

$$\Delta oxy_j(t) \coloneqq \frac{\Delta oxy_j(t) - \mu_j^{\Delta oxy}}{\sigma_j^{\Delta oxy}},\ \Delta deoxy_j(t) \coloneqq \frac{\Delta deoxy_j(t) - \mu_j^{\Delta deoxy}}{\sigma_j^{\Delta deoxy}}. \tag{2}$$

Then the global reference is applied as

$$\Delta oxy_j(t) \coloneqq \Delta oxy_j(t) - \sum_{l=1}^{n} \Delta oxy_l(t),\ \Delta deoxy_j(t) \coloneqq \Delta deoxy_j(t) - \sum_{l=1}^{n} \Delta deoxy_l(t), \tag{3}$$

where n is the number of channels.

To justify the use of the mean and SD in the preparation phase for the z-score conversion in the analysis phase, it is supposed that the preparation phase is sufficiently long and the tasks in the two phases are qualitatively the same.

Local Reference. *Local reference* method is similar to the global reference method, but instead of the average over all channels, it uses average of neighboring channels for the reference:

$$\Delta oxy_j(t) \coloneqq \Delta oxy_j(t) - \sum_{l \in N_j} \Delta oxy_l(t)\,,\ \Delta deoxy_j(t) \coloneqq \Delta deoxy_j(t) - \sum_{l \in N_j} \Delta deoxy_l(t)\,, \tag{4}$$

where N_j denotes the neighboring channels of j. This method is expected to emphasize localized activity, like the Gabor convolution kernel.

Although there are no objective criteria to define the range of the "local" neighbors, we used the nearest neighboring channels (that means $N_1 = \{5,6\}$ and $N_{12} = \{7,8,16,17\}$, etc. in the configuration of Fig. 1).

Independent Component Analysis. *Independent component Analysis* (ICA) assumes that the observed data $x(t) = \left[x_1(t), \ldots x_n(t)\right]$ $(t = 1,2,\ldots,p)$ is a linear combination of unknown and statistically independent sources $s(t) = \left[s_1(t), \ldots, s_m(t)\right]$ $(m \le n)$, that is

$$x(t) = s(t)A\,, \tag{5}$$

where the $m \times n$ matrix A is called *mixing matrix*. The problem for ICA algorithms is to find a *demixing matrix* W, such that the source signals $s(t)$ are recovered from the observed data $x(t)$ by

$$s(t) = x(t)W\,, \tag{6}$$

with maximal statistical independence among the source components.

If it is reasonable to suppose that artifact components are statistically independent from the components originating from cortical activity, the artifacts are eliminated by (i) demixing the observed data into the independent sources, (ii) eliminating source components with characteristic feature for expected artifacts, and (iii) re-mixing the remaining source components (this step is optional for some BCI applications). This procedure is expressed as

$$x(t) \coloneqq x(t)WA'\,, \tag{7}$$

where A' is the modified mixing matrix of A, which is obtained by substituting zeros for the rows corresponding to the artifact components.

ICA has also been widely used for the artifact reduction in various brain recording methods, where physiological/technical artifact components were identified by checking the components' inconsistency with experimental design [14], correlation with external references like electrocardiogram (ECG), or frequency/spatial distribution [15]. For fNIRS [7], Kohno et al. speculated that the skin blood flow artifact tends to be distributed uniformly in wide spatial range, as it is controlled by the autonomic nervous system. Based on this hypothesis, they defined a statistical value named *coefficient of spatial uniformity* (CSU) for each independent component i, as

$$csu_i = \left|\mu(A_{i*})\right| / \sigma(A_{i*})\,, \tag{8}$$

where $\mu(A_{i*})$ and $\sigma(A_{i*})$ are the mean and SD of the mixing matrix A's row i, respectively. Components with high CSU show spatially uniform changes and thus are considered as artifacts.

For real-time analysis, artifact components must be automatically identified based on some predefined criteria. In this study, we adopted the CSU and *cardiac pulsation frequency ratio* (CPFR), which we calculated as integration of the spectral density in frequency region [0.75, 1.5] Hz divided by the total spectral power. ICA was applied separately for (Δoxy_j) and $(\Delta deoxy_j)$, and components with highest CSU and CPFR are eliminated respectively by the above procedure (7). We supposed that the source contains as many dimensions as the observation ($m = n$), and adopted joint approximate diagonalization of eigen-matrices (JADE) for ICA algorithm, which is based on the fourth-order cumulant [16].

Combined Methods. The high-pass filter is applied independently for each channel. On the other hand, the latter three methods employ inter-channel comparison, based on the shared hypothesis that the artifacts in fNIRS signals, mainly from skin blood flow, are not restricted in a specific channel but distributed throughout the channels. Therefore, it can be expected that these two types of methods can complement each other. Based on this idea, we tried three combined methods, which are obtained by first passing the data through the high-pass filter and then applying one of the other three methods.

3 Experiment

We conducted a preliminary experiment to compare the effectiveness of the above methods. In this experiment, each method's effectiveness for artifact reduction was evaluated by improvement in task recognition performance by a classification algorithm.

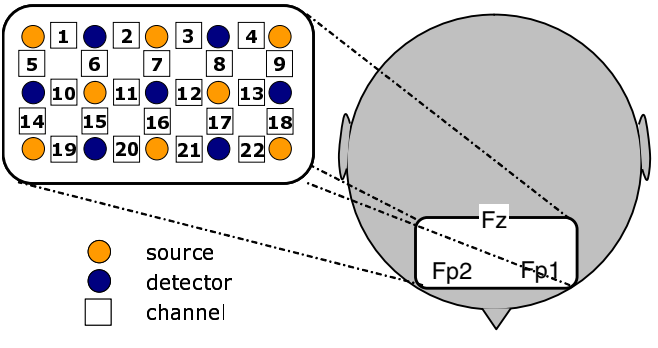

Fig. 1. Configuration of source and detector optodes used in the experiment. For each neighboring pair of source and detector optodes, a recording channel is assigned.

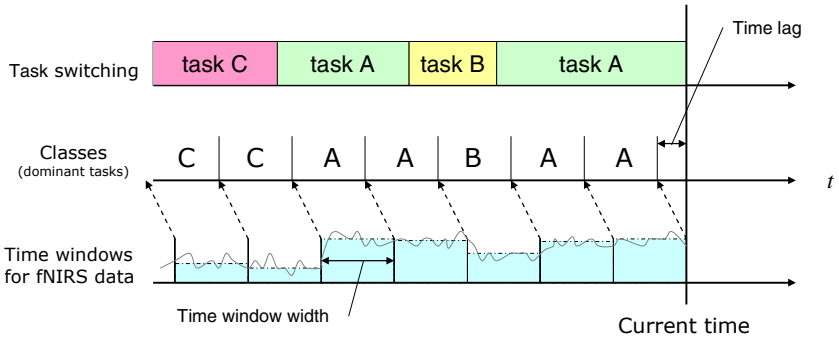

Fig. 2. Construction of feature vectors from fNIRS data, and determination of their classes. For each feature vector, corresponding class is given by the most dominant cognitive task in the lagged time window.

3.1 Settings

Four subjects conducted three types of cognitive tasks which were switched repeatedly in an order defined by the experimenter. The tasks assigned to each subject are shown in Table 1. Every task continued for 15-25 s (the duration was varied to avoid inducing a specific frequency component), and was repeated 10 times each. Subjects were asked to suppress task-dependent postural changes.

Table 1. Assignment of cognitive tasks to the subjects

Subject	Tasks
Subject A	Listening quiet instrumental music, silent text reading, number puzzle (Sudoku).
Subject B	Listening quiet instrumental music, silent text reading, 3D block puzzle.
Subject C	Listening quiet instrumental music, silent text reading, 3D block puzzle.
Subject D	Rest with eyes open, metal arithmetic, typing text using keypad.

We placed 8 source and 7 detector optodes, covering prefrontal regions (including Fp1, Fp2 and Fz positions of the international 10-20 system of EEG electrode placement [17]), by 22 channels. The configuration of optodes is shown in Fig. 1.

For the training and testing of task classifier, 44 dimensional feature vectors were constructed by averaging Δoxy_j and $\Delta deoxy_j$ signals within shifting time windows. Different time window widths ranging from 1 to 10 s (interval 0.5 s) were tried. Considering relatively slow nature of fNIRS response, we also tried various lengths of time lag, ranging from 0 to 10 s (interval 0.5 s), in linking each feature vector to one of the cognitive tasks. Feature vector at the current time was linked to a task which was most dominant in the window shifted to the past by the time lag, as shown in Fig.2. Data in the former half of the experimental period were used for training of the classifier, calculation of mean and SD which were used in z-score conversion for the global/local references, and estimation of the demixing/mixing matrices for the ICA based method. Data in the latter half were used for classification performance test.

Table 2. Task classification precision with no artifact reduction (none), reduction methods based on high-pass filter (HPF), global reference (GR), local reference (LR), independent component analysis (ICA), and their combinations. For each subject and artifact reduction method, the best precision with the time window width (w.w.) and lag values yielding it, average precision (Avg.) ± SD over all the time window widths from 1 to 10 s and lags from 0 to 10 s, and precision at 1 s window width and 0 s lag (At (1, 0)), are shown.

	Method	Best	(w.w., lag)	Avg.	±	SD	At (1, 0)
Subject A	None	0.525	(5.0, 5.0)	0.434	±	0.041	0.428
	HPF	0.651	(4.5, 7.5)	0.519	±	0.057	0.424
	GR	0.595	(7.0, 0.5)	0.446	±	0.047	0.444
	LR	0.579	(3.0, 8.0)	0.468	±	0.052	0.444
	ICA	0.524	(7.0, 0.5)	0.421	±	0.037	0.385
	HPF+GR	0.794	(8.5, 4.0)	0.575	±	0.060	0.572
	HPF+LR	0.689	(6.5, 6.0)	0.554	±	0.050	0.556
	HPF+ICA	0.630	(5.5, 2.0)	0.504	±	0.059	0.576
Subject B	None	0.613	(9.5, 2.5)	0.447	±	0.086	0.469
	HPF	0.800	(8.5, 1.5)	0.583	±	0.077	0.601
	GR	0.646	(3.5, 2.5)	0.391	±	0.092	0.360
	LR	0.718	(7.5, 8.0)	0.475	±	0.097	0.465
	ICA	0.581	(9.5, 0.0)	0.411	±	0.077	0.349
	HPF+GR	0.857	(8.5, 2.5)	0.638	±	0.081	0.640
	HPF+LR	0.844	(6.5, 6.0), (6.5, 6.5)	0.662	±	0.073	0.636
	HPF+ICA	0.800	(8.5, 0.5), (8.5, 1.5)	0.599	±	0.079	0.628
Subject C	None	0.730	(8.0, 7.5)	0.587	±	0.049	0.615
	HPF	0.719	(9.5, 5.0)	0.558	±	0.056	0.576
	GR	0.781	(9.5, 0.0)	0.605	±	0.056	0.599
	LR	0.757	(8.0, 9.0)	0.574	±	0.065	0.469
	ICA	0.714	(8.5, 6.5)	0.594	±	0.049	0.637
	HPF+GR	0.714	(8.5, 6.5)	0.563	±	0.059	0.561
	HPF+LR	0.750	(9.5, 4.0), (9.5, 4.5)	0.622	±	0.046	0.599
	HPF+ICA	0.676	(9.0, 0.0)	0.561	±	0.046	0.588
Subject D	None	0.606	(9.0, 2.5)	0.436	±	0.048	0.508
	HPF	0.533	(10.0, 2.5)	0.369	±	0.056	0.373
	GR	0.697	(9.0, 5.0)	0.523	±	0.056	0.538
	LR	0.650	(7.5, 0.0), (7.5, 1.0)	0.502	±	0.058	0.515
	ICA	0.600	(7.5, 0.0)	0.437	±	0.046	0.562
	HPF+GR	0.571	(7.0, 6.0)	0.415	±	0.047	0.381
	HPF+LR	0.609	(6.5, 1.0)	0.440	±	0.065	0.423
	HPF+ICA	0.514	(8.5, 4.0)	0.391	±	0.044	0.385

For the classification, we adopted nonlinear support vector machine (SVM) algorithm with Gaussian radial basis kernel and the one-against-one method for multiclass-classification [18]. The kernel width parameter was determined heuristically from the training data [19].

3.2 Results

Table 2 shows task classification precision with and without the artifact reduction methods. For each subject and artifact reduction method, the best precision value with the time window width and lag values yielding it, average precision ± SD over all the time window width and lag parameter values, and precision at 1 s window width and 0 s lag, are given. Fig. 3 shows difference of the classification precision by the artifact reduction methods for a subject (subject B), with detailed dependence on the time window width and lag.

For subject A and B, most of the methods were effective in improving task classification precision. Especially the high-pass filter and its combinations with other methods brought significant improvements. Although the ICA based method was not much effective by itself, it achieved fair improvement combined with the high-pass filter. On the other hand, for subject C and D, the high-pass filter and combined

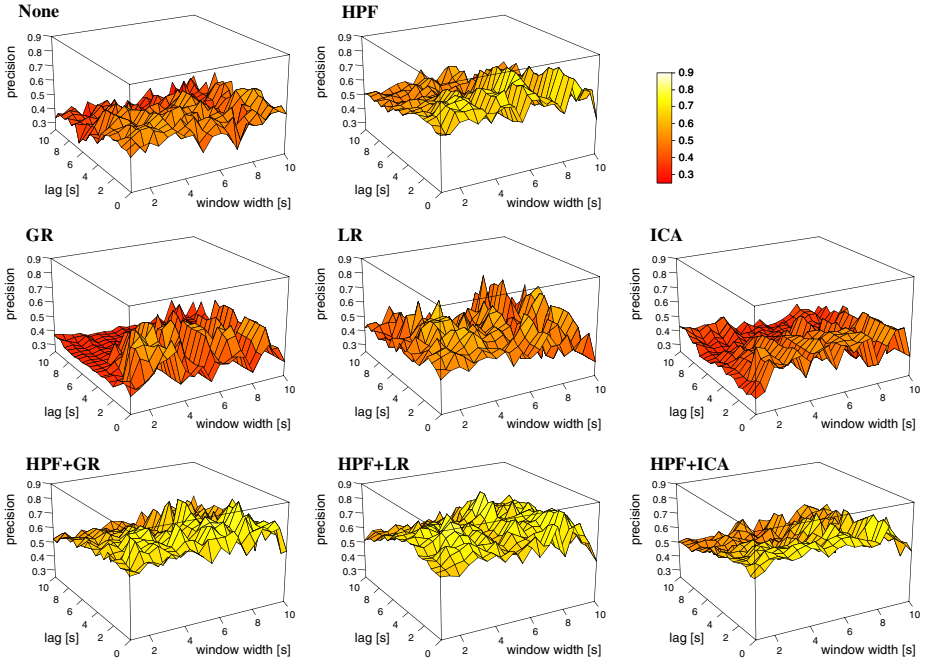

Fig. 3. Detailed dependence of the task classification precision for a subject (subject B) on the time window width and lag, with no artifact reduction (none), reduction methods based on high-pass filter (HPF), global reference (GR), local reference (LR), independent component analysis (ICA), and their combinations.

methods were not very effective and in some cases even diminished the precision. The global reference was comparatively effective for these two subjects.

These results suggest the possibility that for each task (application) and subject (user) we should try out all the methods in some "general artifact reduction package" and chose the best one, rather than pursuing a single standardized method. Such a package can be also utilized for adaptive boosting algorithm [20], to prepare a collection of "weak" classifiers. Our study provides a starting point to assemble such a package.

4 Conclusions

As artifact reduction methods for real-time analysis of fNIRS data, we compared high-pass filtering, global and local average references, independent component analysis based method, and their combinations. Their effectiveness was evaluated by a cognitive task recognition experiment. The results showed all the methods have artifact reduction capability, but their effectiveness depends on subjects and tasks. This suggests that it can be more practical to try various artifact reduction methods and chose the best one for each task and subject, instead of pursuing a single standardized method.

We studied the effectiveness of the methods in an experiment where the tasks were switched in a block-design fashion and thus each cognitive state is expected to continue for relatively long time. For future work, we are planning to compare the artifact reduction methods for quicker responses in the event-related BCI scheme, with real-time biofeedback of the analysis results to the subjects.

Acknowledgments. This study was in part supported by "Symbiotic Information Technology Research Project" of Tokyo University of Agriculture and Technology, and also by the Grant-in-Aid for "Scientific Research on Priority Areas (Area No. 454)" from the Japanese Ministry of Education, Culture, Sports, Science and Technology.

References

1. Koizumi, H., et al.: Present and Future of Brain Imaging in Mind, Brain and Education. In: IMBES Conference (2007)
2. Tamura, H., et al.: On Physiological Role of Quick Components in Near Infrared Spectroscopy. In: MOBILE 2008 (2008)
3. Obrig, H., et al.: Spontaneous Low Frequency Oscillations of Cerebral Hemodynamics and Metabolism in Human Adults. NeuroImage 12, 623–639 (2000)
4. Katura, T., et al.: Quantitative evaluation of interrelations between spontaneous low-frequency oscillations in cerebral hemodynamics and systemic cardiovascular dynamics. NeuroImage 31, 1592–1600 (2006)
5. Hoshi, Y., Tamura, M.: Detection of dynamic changes in cerebral oxygenation coupled to neuronal function during mental work in man. Neurosci. Lett. 150, 5–8 (1993)
6. Matcher, S.J., et al.: Performance Comparison of Several Published Tissue Near-infrared spectroscopy algorithms. Anal. Biochem. 227, 54–68 (1995)

7. Kohno, S., et al.: Removal of the Skin Blood Flow Artifact in Functional Near-infrared Spectroscopic Imaging Data through Independent Component Analysis. Journal of Biomedical Optics 12, 062111–1–9 (2007)
8. Schroeter, M.L., et al.: Towards a Standard Analysis for Functional Near-infrared Imaging. NeuroImage 21, 283–290 (2004)
9. Huppert, T., et al.: A Temporal Comparison of BOLD, ASL, and NIRS Hemodynamic responses to motor stimuli in adult humans. NeuroImage 29, 368–382 (2006)
10. Plichta, M., et al.: Event-Related Functional Near-infrared Spectroscopy (fNIRS): Are the Measurements Reliable? NeuroImage 31, 116–124 (2006)
11. Proakis, J., Manolakis, D.: Digital Signal Processing. Prentice Hall, Englewood Cliffs (2006)
12. Bénar, C., et al.: Single-Trial Analysis of Oddball Event-Related Potentials in Simultaneous EEG-fMRI. Human Brain Mapping 28, 602–613 (2007)
13. Matsuda, G., Hiraki, K.: Sustained Decrease in Oxygenated Hemoglobin during Video Games in the Dorsal Prefrontal Cortex: A NIRS Study of Children. NeuroImage 29, 706–711 (2006)
14. Ikeda, S., Toyama, K.: Independent Component Analysis for Noisy Data — MEG Data Analysis. Neural Networks 13, 1063–1074 (2000)
15. Mantini, D., et al.: Complete Artifact Removal for EEG Recorded during Continuous fMRI Using Independent Component Analysis. NeuroImage 34, 598–607 (2007)
16. Cardoso, J.-F., Souloumiac, A.: Blind Beamforming for Non Gaussian Signals. IEEE Proceedings-F 140, 362–370 (1993)
17. Homan, R.W., Herman, J., Purdy, P.: Cerebral location of international 10-20 system electrode placement. Electroencephalogr. Clin. Neurophysiol. 66, 376–382 (1987)
18. Hsu, C.-W., Lin, C.-J.: A Comparison of Methods for Multiclass Support Vector Machines. IEEE Trans. Neural Networks 13, 415–425 (2002)
19. Karatzoglou, A., Meyer, D., Hornik, K.: Support Vector Machines in R. Journal of Statistical Software 16(9) (2006)
20. Freund, Y., Schapier, R.E.: A Decision-Theoretic Generalization of On-line Learning and an Application to Boosting. Journal of Computer and System Sciences 55, 119–139 (1997)